International Journal of Control, Automation, and Systems (2015) 13(3):587-594
DOI 10.1007/s12555-014-0249-3

ISSN:1598-6446 eISSN:2005-4092
http://www.springer.com/12555

Adaptive Leader-follower Formation Control of Mobile Robots with Unknown Skidding and Slipping Effects

Bong Seok Park and Sung Jin Yoo*

Abstract: This paper investigates an adaptive leader-follower formation control problem of multiple mobile robots in the presence of unknown skidding and slipping. First, we employ the concept of virtual robots to achieve the desired formation and derive the kinematics of the virtual leader and follower robots considering skidding and slipping effects. Then, we design an adaptive formation controller based on a two-dimensional error surface where the adaptive technique is used for compensating the unknown skidding and slipping effects that influence the follower robots. From Lyapunov stability theorem, we show that all errors of the closed-loop system are uniformly ultimately bounded, and thus the desired formation is successfully achieved regardless of the presence of unknown skidding and slipping effects. Simulation results are provided to demonstrate the effectiveness of the proposed formation control scheme.

Keywords: Adaptive control, formation control, leader-follower approach, mobile robots, skidding and slipping effects.

1. INTRODUCTION

During the past few years, many studies have been conducted on mobile robots with focus on solving various control problems, such as the tracking problem at the kinematic level [1,2], the tracking problem at the dynamic level [3,4], the tracking problem at the actuator level [5], and the unified tracking and stabilization problem [6,7]. All these studies assumed that the wheels of mobile robots purely roll and do not slip. However, in practice, this assumption may not be reasonable owing to environmental factors such as the road condition (i.e., an icy or wet road) and the tire deformation. Thus, the application of the controllers developed for solving the above-listed control problems to mobile robots with skidding and slipping may be problematic. Motivated by this observation, the control problem in the presence of skidding and slipping effects has been regarded as an attractive research topic [8-13]. In [10], the models of wheeled mobile robots considering both the skidding and the slipping of the wheels were proposed and the controllability according to the maneuverability of mobile robots was analyzed. Further, the authors of [11,12] designed path following and tracking controllers for mobile robots by considering skidding and slipping effects. In [13], the author considered an adaptive control problem in order to address unknown skidding and slipping effects. However, all these works [8-13] allowed for the control of only single mobile robots with skidding and slipping effects. In other words, the results cannot be applied to the formation control of multiple mobile robots due to the coupling problems in the formation dynamics when considering the skidding and slipping effects.

On the other hand, the formation control of multiple mobile robots has gained an increasing interest from the control theory community owing to various applications such as cooperative transportation, reconnaissance, search, and so on. In the literature, popular formation control methods are fourfold: behavior-based control [14,15], graph theory [16,17], virtual structure [18-20], and leader-follower approach [21,22]. Among these approaches, the leader-follower approach has been largely studied by many researchers because it is easy to understand mathematically and shows good scalability. In its early days of research on mobile robots, the studies were performed at the kinematic level of mobile robots [21]. The formation control systems including collision avoidance were proposed in [23,24] and the adaptive leader-follower formation controller in the absence of the leader's velocity information was designed in [25]. The distributed formation control law which does not use global position measurements was proposed in [26]. For more practical applications, many studies have been conducted at the dynamic level of mobile robots. The sliding mode formation controller was proposed in [27,28] and the neural network control method was used for the leader-follower-based robot formations [29-31]. Moreover, a formation control design considering the actuator dynamics was presented in [32,33]. However, none of all these works related to the leader-follower

Manuscript received June 20, 2014; revised July 23, 2014; accepted August 2, 2014. Recommended by Associate Editor Ho Jae Lee under the direction of Editor Euntai Kim.

This study was supported by research fund from Chosun University, 2015.

Bong Seok Park is with the Department of Electronic Engineering, Chosun University, 309 Pilmun-daero, Dong-gu, Gwang ju 501-759, Korea (e-mail: bspark@chosun.ac.kr).

Sung Jin Yoo is with the School of Electrical and Electronics Engineering, Chung-Ang University, 84 Heukseok-ro, Dongjak-gu, Seoul 156-756, Korea (e-mail: sjyoo@cau.ac.kr).

* Corresponding author.

formation control addressed the skidding and slipping effects of wheels of mobile robots. To the best of our knowledge, there have been no research results available on the leader-follower-based formation control problem of mobile robots in the presence of skidding and slipping effects.

Accordingly, we propose an adaptive leader-follower formation control approach for a class of multiple mobile robots with unknown skidding and slipping. In order to design the formation controller, a leader-follower model considering skidding and slipping effects is newly derived. Then, a two-dimensional error surface consisting of position and orientation errors is presented to design the formation controller. In the controller design, the adaptive technique is successfully applied to compensate the unknown skidding and slipping effects that influence the follower robots, regardless of the coupling problems among model nonlinearities and the skidding and slipping effects. From Lyapunov stability theorem, it is proved that all error signals of the closed-loop system are uniformly ultimately bounded, all point tracking errors converge to an adjustable neighborhood of the origin. Furthermore, the convergence of the orientation error is analyzed from the relationship between the robots' velocities and the skidding velocity. Finally, simulation results are included to demonstrate the effectiveness of the proposed formation control scheme.

This paper is organized as follows. In Section 2, we introduce the kinematics and dynamics of mobile robots in the presence of skidding and slipping, and derive a leader-follower model considering skidding and slipping. In Section 3, an adaptive formation controller for multiple mobile robots is designed in the presence of unknown skidding and slipping, and the stability of the proposed control system is analyzed. Simulation results are discussed in Section 4. Finally, Section 5 gives some conclusions. Throughout this paper, the following notations are used: 1) $\|\cdot\|$ stands for the Euclidean norm of a vectors; 2) the subscripts 'l' and 'f' represent the leader and the follower, respectively; and 3) diag[·] denotes the diagonal matrix.

2. PROBLEM FORMULATION

2.1. Mobile robot model in the presence of skidding and slipping effects

The kinematics and dynamics of mobile robots in the presence of skidding and slipping effects are described by the following equations [13]

$$\dot{\boldsymbol{q}} = \boldsymbol{J}(\boldsymbol{q})(\boldsymbol{z}-\boldsymbol{\rho}) + \boldsymbol{\varphi}(\boldsymbol{q},\mu), \tag{1}$$

$$\begin{aligned} \boldsymbol{H}(\boldsymbol{q})\dot{\boldsymbol{z}}, = \boldsymbol{H}(\boldsymbol{q})\dot{\boldsymbol{\rho}} - F_1(\boldsymbol{q},\dot{\boldsymbol{q}})(\boldsymbol{z}-\boldsymbol{\rho}) - F_2(\boldsymbol{q})\dot{\boldsymbol{\varphi}}(\boldsymbol{q},\mu) \\ - F_3(\boldsymbol{q})\boldsymbol{\varphi}(\boldsymbol{q},\mu) + \boldsymbol{\tau}, \end{aligned} \tag{2}$$

where

$$\boldsymbol{J}(\boldsymbol{q}) = \begin{bmatrix} \cos\theta & 0 \\ \sin\theta & 0 \\ 0 & 1 \end{bmatrix},$$

$$\boldsymbol{H}(\boldsymbol{q}) = (\boldsymbol{J}^T(\boldsymbol{q})\boldsymbol{B}(\boldsymbol{q}))^{-1}\boldsymbol{J}^T(\boldsymbol{q})\boldsymbol{M}(\boldsymbol{q})\boldsymbol{J}(\boldsymbol{q}),$$

$$\begin{aligned} \boldsymbol{F}_1(\boldsymbol{q},\dot{\boldsymbol{q}}) &= (\boldsymbol{J}^T(\boldsymbol{q})\boldsymbol{B}(\boldsymbol{q}))^{-1} \\ &\quad \times \boldsymbol{J}^T(\boldsymbol{q})\left(\boldsymbol{M}(\boldsymbol{q})\dot{\boldsymbol{J}}(\boldsymbol{q}) + \boldsymbol{C}(\boldsymbol{q},\dot{\boldsymbol{q}})\boldsymbol{J}(\boldsymbol{q})\right), \end{aligned}$$

$$\boldsymbol{F}_2(\boldsymbol{q}) = (\boldsymbol{J}^T(\boldsymbol{q})\boldsymbol{B}(\boldsymbol{q}))^{-1}\boldsymbol{J}^T(\boldsymbol{q})\boldsymbol{M}(\boldsymbol{q}),$$

$$\boldsymbol{F}_3(\boldsymbol{q}) = (\boldsymbol{J}^T(\boldsymbol{q})\boldsymbol{B}(\boldsymbol{q}))^{-1}\boldsymbol{J}^T(\boldsymbol{q})\boldsymbol{C}(\boldsymbol{q},\dot{\boldsymbol{q}}),$$

$$\boldsymbol{M}(\boldsymbol{q}) = \begin{bmatrix} m & 0 & md\sin\theta \\ 0 & m & -md\cos\theta \\ md\sin\theta & -md\cos\theta & I \end{bmatrix},$$

$$\boldsymbol{B}(\boldsymbol{q}) = \frac{1}{r}\begin{bmatrix} \cos\theta & \cos\theta \\ \sin\theta & \sin\theta \\ b & -b \end{bmatrix}, \ \boldsymbol{C}(\boldsymbol{q},\dot{\boldsymbol{q}}) = \begin{bmatrix} 0 & 0 & md\dot{\theta}\cos\theta \\ 0 & 0 & md\dot{\theta}\sin\theta \\ 0 & 0 & 0 \end{bmatrix},$$

$$m = m_c + 2m_w, \quad I = m_c d^2 + 2m_w b^2 + I_c + 2I_m.$$

In these expressions, $2b$ is the width of the mobile robot, r is the radius of the wheel, and d is the distance between the center of mass of the mobile robot and the mid point between the left and right wheels. Further, m_c and m_w are masses of the body and wheel with a motor, resepectively. I_c, I_w, and I_m are moments of inertia of the body about the vertical axis, of the wheel with a motor about the wheel axis, and of the wheel with a motor about the wheel diameter, respectively. $\boldsymbol{q} = [x, y, \theta]^T$; (x, y) are the coordinates of the midpoint between the two driving wheels, and θ is the heading angle of the mobile robot, $\boldsymbol{z} = [v, \omega]^T$; v and ω are the linear velocity and the angular velocity, respectively, of the mobile robot, $\boldsymbol{\rho} = [\rho_1, \rho_2]^T$; ρ_1 is the longitudinal slip velocity and ρ_2 is the yaw rate perturbation due to the slippage of the wheels $\boldsymbol{\varphi}(\boldsymbol{q},\mu) = [-\mu\sin\theta, \mu\cos\theta, 0]^T$; μ is the lateral skidding velocity, and $\boldsymbol{\tau}$ is the control torque applied to the wheels.

Assumption 1: The skidding and slipping perturbations ρ_1, ρ_2, and $\boldsymbol{\varphi}(\boldsymbol{q},\mu)$ are bounded as $|\rho_1| < \zeta_1$, $|\rho_2| < \zeta_2$, and $\|\boldsymbol{\varphi}(\boldsymbol{q},\mu)\| = |\mu| < \zeta_3$ where ζ_i $(i = 1, 2, 3)$ are *unknown* positive constants, and their first derivatives are bounded as $|\dot{\rho}_1| < \zeta_{d1}$, $|\dot{\rho}_2| < \zeta_{d2}$, and $\|\dot{\boldsymbol{\varphi}}(\boldsymbol{q},\mu)\| < \zeta_{d3} + \zeta_3(|\omega| + \zeta_2)$ with $|\dot{\mu}| < \zeta_{d3}$ where ζ_{di} $(i = 1,2,3)$ are *unknown* positive constants.

Remark 1: Assumption 1 is reasonable owing to Property 2 reported in [10]. Unlike the approach in [10], our approach does not require knowledge of the bounds of the skidding and slipping perturbations for designing the formation controller because the unknown bounds are estimated by the adaptive technique. These bounds are only used to prove the stability of the proposed control system.

2.2. Leader-follower model considering skidding and slipping

In this section, we derive the leader-follower model in the presence of skidding and slipping effects and present the adaptive formation control problem based on the leader-follower configuration as shown in Fig. 1. In order

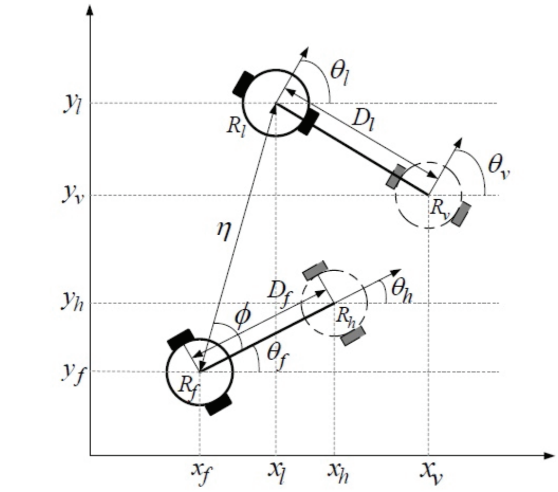

Fig. 1. Leader-follower configuration of two robots.

to achieve the desired formation, we employ the concept of virtual robots instead of using actual robots. In other words, the position $\mathbf{q_v} = [x_v, y_v, \theta_v]^T$ of the virtual leader R_v, which is located at a distance D_l from the center $\mathbf{q_l} = [x_l, y_l, \theta_l]^T$ of the actual leader R_l, is defined as follows:

$$\begin{aligned} x_v &= x_l + D_l \sin\theta_l, \\ y_v &= y_l - D_l \cos\theta_l, \\ \theta_v &= \theta_l, \end{aligned} \tag{3}$$

where $D_l = \eta_d \sin\phi_d$; η_d and ϕ_d are, respectively, the desired distance and angle of the follower with respect to the leader. Then, using the kinematic (1) in the presence of skidding and slipping, the derivative of (3) is obtained as

$$\begin{bmatrix} \dot{x}_v \\ \dot{y}_v \\ \dot{\theta}_v \end{bmatrix} = \begin{bmatrix} \cos\theta_l & D_l \cos\theta_l \\ \sin\theta_l & D_l \sin\theta_l \\ 0 & 1 \end{bmatrix} \begin{bmatrix} v_l - \rho_{1l} \\ \omega_l - \rho_{2l} \end{bmatrix} + \begin{bmatrix} -\mu_l \sin\theta_l \\ \mu_l \cos\theta_l \\ 0 \end{bmatrix}. \tag{4}$$

Similarly, the position $\mathbf{q_h} = [x_h, y_h, \theta_h]^T$ of the virtual follower R_h which is located at a distance D_f from the center $\mathbf{q_f} = [x_f, y_f, \theta_f]^T$ of the actual follower R_f, is expressed as

$$\begin{aligned} x_h &= x_f + D_f \cos\theta_f, \\ y_h &= y_f + D_f \sin\theta_f, \\ \theta_h &= \theta_f, \end{aligned} \tag{5}$$

where $D_f = \eta_d \cos\phi_d$. The derivative of (5) is also represented by

$$\begin{bmatrix} \dot{x}_h \\ \dot{y}_h \\ \dot{\theta}_h \end{bmatrix} = \begin{bmatrix} \cos\theta_f & -D_f \sin\theta_f \\ \sin\theta_f & D_f \sin\theta_f \\ 0 & 1 \end{bmatrix} \begin{bmatrix} v_f - \rho_{1f} \\ \omega_f - \rho_{2f} \end{bmatrix} + \begin{bmatrix} -\mu_f \sin\theta_f \\ \mu_f \cos\theta_f \\ 0 \end{bmatrix}. \tag{6}$$

Assumption 2: The velocities of the leader robot $v_l > 0$, ω_l, and its first derivatives are available and bounded.

Remark 2: Notice that Assumption 2 on the boundedness of the leader's velocity is general and reasonable in the field of leader-follower formation control [23]. In the leader-follower formation scheme, since the leader robot plays the role of a reference robot for the follower robots the follower robot cannot track the leader robot if the leader robot's velocity is not bounded. In addition, $v_l > 0$ means that this study only focuses on the desired formation tracking problem, i.e., we do not consider the problem of stabilization.

The *control objective* is to steer the virtual follower so that it follows the virtual leader, which implies that the actual follower maintains the desired distance and angle with respect to the actual leader in the presence of unknown skidding and slipping effects.

3. MAIN RESULTS

In order to design an adaptive formation controller for mobile robots with skidding and slipping, let us define the tracking errors between R_v and R_h as

$$x_e = x_v - x_h, \quad y_e = y_v - y_h, \quad \theta_e = \theta_v - \theta_h. \tag{7}$$

Then, we consider an error surface $\boldsymbol{s} = [s_1, s_2]^T$ as follows:

$$\boldsymbol{s} = \begin{bmatrix} s_1 \\ s_2 \end{bmatrix} = \begin{bmatrix} -s_x \cos\theta_f - s_y \sin\theta_f \\ s_x \sin\theta_f - s_y \cos\theta_f \end{bmatrix}, \tag{8}$$

where $s_x = \dot{x}_e + kx_e$ and $s_y = \dot{y}_e + ky_e$; $k > 0$ is a design constant. By applying (3)–(6), the derivative of the error dynamics is given by

$$\begin{aligned} \dot{\boldsymbol{s}} &= \begin{bmatrix} \dot{v}_f - \dot{v}_l \cos\theta_e - \dot{\omega}_l D_l \cos\theta_e + \alpha_1 + \beta_1 + \gamma_1 \\ \dot{\omega}_f D_f - \dot{v}_l \sin\theta_e - \dot{\omega}_l D_l \sin\theta_e + \alpha_2 + \beta_2 + \gamma_2 \end{bmatrix} \\ &= \boldsymbol{P}\dot{\boldsymbol{z}}_f - \boldsymbol{PQ}\dot{\boldsymbol{z}}_l + \boldsymbol{\alpha} + \boldsymbol{\beta} + \boldsymbol{\gamma}, \end{aligned} \tag{9}$$

where

$$\boldsymbol{\alpha} = [\alpha_1, \alpha_2]^T, \quad \boldsymbol{\beta} = [\beta_1, \beta_2]^T, \quad \boldsymbol{\gamma} = [\gamma_1, \gamma_2]^T,$$

$$\boldsymbol{P} = \begin{bmatrix} 1 & 0 \\ 0 & D_f \end{bmatrix}, \quad \boldsymbol{Q} = \begin{bmatrix} \cos\theta_e & D_l \cos\theta_e \\ \dfrac{\sin\theta_e}{D_f} & \dfrac{D_l \sin\theta_e}{D_f} \end{bmatrix},$$

$$\begin{aligned} \alpha_1 &= \left(v_l\omega_l + \omega_l^2 D_l - \omega_f v_l - \omega_f \omega_l D_l\right)\sin\theta_e \\ &\quad - k(v_l + \omega_l D_l)\cos\theta_e \\ &\quad + k(x_e\omega_f \sin\theta_f - y_e\omega_f \cos\theta_f + v_f), \end{aligned}$$

$$\begin{aligned} \alpha_2 &= \left(-v_l\omega_l - \omega_l^2 D_l + \omega_f v_l + \omega_f \omega_l D_l\right)\cos\theta_e \\ &\quad + k\left(D_f\omega_f + x_e\omega_f \cos\theta_f + y_e\omega_f \sin\theta_f\right) \\ &\quad - k(v_l + \omega_l D_l)\sin\theta_e, \end{aligned}$$

$$\begin{aligned} \beta_1 &= (\rho_{1l}\rho_{2l} - \rho_{1l}\omega_l - \rho_{2l}v_l + \rho_{2l}^2 D_l - 2\omega_l\rho_{2l}D_l + \dot{\mu}_l \\ &\quad - \rho_{1l}\rho_{2f} + \rho_{2f}v_l - \rho_{2f}\rho_{2l}D_l \\ &\quad + \rho_{2f}\omega_l D_l + k\mu_l)\sin\theta_e \end{aligned}$$

$$
\begin{aligned}
&-\dot{\rho}_{1f} - k\rho_{1f} + (\dot{\rho}_{1l} + \dot{\rho}_{2l}D_l + \mu_l(\omega_l - \rho_{2l}) \\
&\quad + \rho_{2f}\mu_l + k\rho_{1l} + k\rho_{2l}D_l)\cos\theta_e, \\
\beta_2 &= (-\rho_{1l}\rho_{2l} + \rho_{1l}\omega_l + \rho_{2l}v_l + 2\rho_{2l}\omega_l D_l - \rho_{2l}^2 - \dot{\mu}_l \\
&\quad - \rho_{2f}v_l + \rho_{2f}\rho_{1l} - \rho_{2f}\omega_l D_l \\
&\quad + \rho_{2f}\rho_{2l}D_l - k\mu_l)\cos\theta_e \\
&\quad - \dot{\rho}_{2f}D_f + \dot{\mu}_f - kD_f\rho_{2f} + k\mu_f \\
&\quad + (\dot{\rho}_{1l} + \dot{\rho}_{2l}D_l + \mu_l(\omega_l - \rho_{2l} + \rho_{2f}) \\
&\quad + k\rho_{1l} + kD_l\rho_{2l})\sin\theta_e, \\
\gamma_1 &= (\rho_{1l} + \rho_{2l}D_l)\omega_f \sin\theta_e - kx_e\rho_{2f}\sin\theta_f \\
&\quad + ky_e\rho_{2f}\cos\theta_f, \\
\gamma_2 &= -(\rho_{1l} + \rho_{2l}D_l)\omega_f\cos\theta_e - kx_e\rho_{2f}\cos\theta_f \\
&\quad - ky_e\rho_{2f}\sin\theta_f - \mu_l\omega_f\sin\theta_e.
\end{aligned}
$$

Here, $\boldsymbol{\gamma}$ is expressed by the vector form $\boldsymbol{\gamma} = \boldsymbol{W}\Phi$ where $\boldsymbol{\Phi} = [\omega_f, x_e, y_e]^T$ and

$$
\boldsymbol{W} = \begin{bmatrix} \varrho\sin\theta_e & -k\rho_{2f}\sin\theta_f & k\rho_{2f}\cos\theta_f \\ -\varrho\cos\theta_e - \mu_l\sin\theta_e & -k\rho_{2f}\cos\theta_f & k\rho_{2f}\sin\theta_f \end{bmatrix}
$$

with $\varrho = \rho_{1l} + \rho_{2l}D_l$.

Remark 3: In (9), $\boldsymbol{\alpha}$ is the known vector, and $\boldsymbol{\beta}$ and $\boldsymbol{W}$ in $\boldsymbol{\gamma}$ are unknown bounded vector and matrix, respectively, resulting from the unknown skidding and slipping effects of both the leader and the follower robots. Therefore, the vector $\boldsymbol{\beta}$ and the matrix $\boldsymbol{W}$ in $\boldsymbol{\gamma}$ are tuned by the adaptive technique.

The control input $\boldsymbol{\tau}_f$ of the follower robot is chosen as

$$
\begin{aligned}
\boldsymbol{\tau}_f &= \boldsymbol{H}(\boldsymbol{q}_f)\boldsymbol{u}_f, \\
\boldsymbol{u}_f &= N_1\boldsymbol{z}_f + \boldsymbol{Q}\dot{\boldsymbol{z}}_l - \boldsymbol{P}^{-1}\boldsymbol{\alpha} - \boldsymbol{R}\boldsymbol{s} - \boldsymbol{N}\hat{\boldsymbol{\delta}},
\end{aligned} \tag{10}
$$

where

$$
\begin{aligned}
\boldsymbol{N} &= \left[\frac{N_1N_1^T\boldsymbol{s}}{2\epsilon}, \frac{N_2N_2^T\boldsymbol{s}}{2\epsilon}, \frac{N_3N_3^T}{2\epsilon}, \frac{\boldsymbol{s}}{2\epsilon}, \frac{\boldsymbol{s}\,\|\Phi\|^2}{2\epsilon}\right], \\
N_1 &= \boldsymbol{H}^{-1}(\boldsymbol{q}_f)F_1(\boldsymbol{q}_f, \dot{\boldsymbol{q}}_f), \quad N_2 = \boldsymbol{H}(\boldsymbol{q}_f)^{-1}F_2(\boldsymbol{q}_f), \\
N_3 &= \boldsymbol{H}(\boldsymbol{q}_f)^{-1}F_3(\boldsymbol{q}_f), \quad \boldsymbol{R} = \mathrm{diag}[r_1, r_2] > 0,
\end{aligned}
$$

ϵ is a positive constant, and $\hat{\boldsymbol{\delta}} = [\hat{\delta}_1, \hat{\delta}_2, \hat{\delta}_3, \hat{\delta}_4, \hat{\delta}_5]^T$ is the estimate of $\boldsymbol{\delta} = [\delta_1, \delta_2, \delta_3, \delta_4, \delta_5]^T$. Here,

$$
\begin{aligned}
&\delta_1 = \zeta_{1f}^2 + \zeta_{2f}^2, \quad \delta_2 = \zeta_{d3,f} + \zeta_{3f}(|\omega_f| + \zeta_{2f}), \\
&\delta_3 = \zeta_{3f}, \quad \delta_4 = (\zeta_{d1,f} + (1/D_f)\bar{\beta}_1)^2 + (\zeta_{d2,f} + \bar{\beta}_2)^2
\end{aligned}
$$

with $|\beta_1| \le \bar{\beta}_1$ and $|\beta_2| \le \bar{\beta}_2$, and

$$
\begin{aligned}
\delta_5 &= 2(k\zeta_{2f})^2(1/D_f^2 + 1) + (1/D_f^2)(\zeta_{1l} + \zeta_{2l}D_l)^2 \\
&\quad + (\zeta_{1l} + \zeta_{2l}D_l + \zeta_{3l})^2.
\end{aligned}
$$

The adaptive parameter vector $\hat{\boldsymbol{\delta}}$ is tuned by the following adaptive law

$$
\dot{\hat{\boldsymbol{\delta}}} = \Lambda\boldsymbol{N}^T\boldsymbol{s} - \sigma\Lambda\hat{\boldsymbol{\delta}}, \tag{11}
$$

where $\Lambda = \mathrm{diag}[\lambda_1, \lambda_2, \lambda_3, \lambda_4, \lambda_5] > 0$ and σ is a positive small gain for the σ-modification [34].

Remark 4: The term $\mathbf{P}^{-1}$ in the control input (10) has the singularity problem when $\phi_d = \pm\pi/2$. To avoid this problem, we use the following perturbed version instead of ϕ_d for this special circumstance:

$$
\bar{\phi}_d = \phi_d + \varepsilon, \tag{12}
$$

where $\varepsilon \ne 0$ is a sufficiently small constant. This version is generally used in the field of formation control using the concept of a virtual leader and follower [23].

Theorem 1: Consider the follower mobile robot (1) and (2) with unknown skidding and slipping that is controlled by the proposed controller (10) with the adaptive law (11). If the proposed control system satisfies Assumptions 1 and 2, then the point tracking errors (x_e, y_e) converge to an adjustable neighborhood of the origin and the orientation error satisfies $\lim_{t\to\infty}[\sin\theta_e - (D_f\dot{\theta}_f + \mu_f)/(v_l + D_l\dot{\theta}_l - \rho_{1l} + \mu_l)] \le \varpi$ where ϖ is a constant that can be arbitrarily small. Further, if the follower robot does not rotate (i.e., $\dot{\theta}_f = 0$) and its lateral skidding velocity μ_f is $\mu_f = 0$, the orientation error θ_e converges to an adjustable neighborhood of the origin, while all signals of the controlled closed-loop system are uniformly ultimately bounded. Thus, the formation errors x_e, y_e, and θ_e are bounded and the desired formation is achieved successfully.

Proof: From the dynamics (2) for the follower robot, we can obtain the following equation

$$
\dot{\boldsymbol{z}}_f = \dot{\boldsymbol{\rho}}_f - N_1(\boldsymbol{z}_f - \boldsymbol{\rho}_f) - N_2\dot{\boldsymbol{\varphi}}_f - N_3\boldsymbol{\varphi}_f + \boldsymbol{u}_f. \tag{13}
$$

Substituting (13) into (9) yields

$$
\begin{aligned}
\dot{\boldsymbol{s}} &= \boldsymbol{P}\left(\dot{\boldsymbol{\rho}}_f - N_1(\boldsymbol{z}_f - \boldsymbol{\rho}_f) - N_2\dot{\boldsymbol{\varphi}}_f - N_3\boldsymbol{\varphi}_f + \boldsymbol{u}_f\right) \\
&\quad - \boldsymbol{P}\boldsymbol{Q}\dot{\boldsymbol{z}}_l + \boldsymbol{\alpha} + \boldsymbol{\beta} + \boldsymbol{W}\Phi.
\end{aligned} \tag{14}
$$

Consider the following Lyapunov function candidate

$$
V = \frac{1}{2}\left(\boldsymbol{s}^T\boldsymbol{P}^{-1}\boldsymbol{s} + \tilde{\boldsymbol{\delta}}^T\Lambda^{-1}\tilde{\boldsymbol{\delta}}\right), \tag{15}
$$

where $\tilde{\boldsymbol{\delta}} = \boldsymbol{\delta} - \hat{\boldsymbol{\delta}}$.

The time derivative of (15) along with (14) is

$$
\begin{aligned}
\dot{V} &= \boldsymbol{s}^T\boldsymbol{P}^{-1}\dot{\boldsymbol{s}} - \tilde{\boldsymbol{\delta}}^T\Lambda^{-1}\dot{\hat{\boldsymbol{\delta}}} \\
&= \boldsymbol{s}^T\{\dot{\boldsymbol{\rho}}_f - N_1(\boldsymbol{z}_f - \boldsymbol{\rho}_f) - N_2\dot{\boldsymbol{\varphi}}_f - N_3\boldsymbol{\varphi}_f \\
&\quad + \boldsymbol{u}_f - \boldsymbol{Q}\dot{\boldsymbol{z}}_l + \boldsymbol{P}^{-1}(\boldsymbol{\alpha} + \boldsymbol{\beta} + \boldsymbol{W}\Phi)\} - \tilde{\boldsymbol{\delta}}^T\Lambda^{-1}\dot{\hat{\boldsymbol{\delta}}}.
\end{aligned} \tag{16}
$$

Using (10), (11), and Young's inequality, (16) can be rewritten as

$$
\begin{aligned}
\dot{V} &= \boldsymbol{s}^T\{\dot{\boldsymbol{\rho}}_f + N_1\boldsymbol{\rho}_f - N_2\dot{\boldsymbol{\varphi}}_f - N_3\boldsymbol{\varphi}_f - \boldsymbol{R}\boldsymbol{s} - \boldsymbol{N}\hat{\boldsymbol{\delta}} \\
&\quad + \boldsymbol{P}^{-1}(\boldsymbol{\beta} + \boldsymbol{W}\Phi)\} - \tilde{\boldsymbol{\delta}}^T\{\boldsymbol{N}^T\boldsymbol{s} - \sigma\hat{\boldsymbol{\delta}}\}
\end{aligned}
$$

$$\begin{aligned}
&\le -\boldsymbol{s}^T\boldsymbol{R}\boldsymbol{s} + \|\boldsymbol{s}^T N_1\|\|\boldsymbol{\rho}_f\| + \|\boldsymbol{s}^T N_2\|\|\dot{\boldsymbol{\varphi}}_f\| \\
&\quad + \|\boldsymbol{s}^T N_3\|\|\boldsymbol{\varphi}_f\| + \|\boldsymbol{s}\|\|\dot{\boldsymbol{\rho}}_f + \boldsymbol{P}^{-1}\boldsymbol{\beta}\| \\
&\quad + \|\boldsymbol{s}^T \boldsymbol{P}^{-1}\boldsymbol{W}\Phi\| - \boldsymbol{s}^T\boldsymbol{N}\hat{\boldsymbol{\delta}} - \tilde{\boldsymbol{\delta}}^T\{\boldsymbol{N}^T\boldsymbol{s} - \sigma\hat{\boldsymbol{\delta}}\} \\
&\le -\boldsymbol{s}^T\boldsymbol{R}\boldsymbol{s} + \delta_1\frac{\boldsymbol{s}^T N_1 N_1^T \boldsymbol{s}}{2\epsilon} + \delta_2\frac{\boldsymbol{s}^T N_2 N_2^T \boldsymbol{s}}{2\epsilon} \\
&\quad + \delta_3\frac{\boldsymbol{s}^T N_3 N_3^T \boldsymbol{s}}{2\epsilon} + \delta_4\frac{\boldsymbol{s}^T\boldsymbol{s}}{2\epsilon} + \delta_5\frac{\|\boldsymbol{s}\|^2\|\Phi\|^2}{2\epsilon} - \boldsymbol{s}^T\boldsymbol{N}\hat{\boldsymbol{\delta}} \\
&\quad - \tilde{\boldsymbol{\delta}}^T\{\boldsymbol{N}^T\boldsymbol{s} - \sigma\hat{\boldsymbol{\delta}}\} + \frac{5}{2}\epsilon \\
&\le -\boldsymbol{s}^T\boldsymbol{R}\boldsymbol{s} - \frac{\sigma}{2}\tilde{\boldsymbol{\delta}}^T\tilde{\boldsymbol{\delta}} + \frac{\sigma}{2}\|\boldsymbol{\delta}\|^2 + \frac{5}{2}\epsilon \\
&\le -2c_1 V + c_2,
\end{aligned}$$

where $0 < c_1 < \min\{r_1, D_f r_2, (\sigma/2)\Lambda_{min}\}$, $c_2 = (\sigma/2)\|\delta\|^2 + (5/2)\epsilon$, and Λ_{min} is a minimum eigenvalue of Λ. Multiplying $e^{2c_1 t}$ and integrating it over $[0, t]$ yield

$$0 \le V(t) \le \frac{c_2}{2c_1} + \left[V(0) - \frac{c_2}{2c_1}\right]e^{-2c_1 t}. \tag{18}$$

In (18), $V(t)$ is bounded by $(c_2/2c_1)$ as time goes to infinity. Therefore, all error signals $\boldsymbol{s}$ and $\tilde{\boldsymbol{\delta}}$ are uniformly ultimately bounded. Moreover, the bound $(c_2/2c_1)$ can be made arbitrarily small by adjusting $\boldsymbol{R}$, Λ, σ, and ε. This means that x_e, y_e, $\dot{x}_e$, and $\dot{y}_e$ converge to an adjustable neighborhood of the origin.

Now, we prove the boundedness of θ_e. From (4) and (6), we can obtain the following equations

$$\begin{aligned}
\sin\theta_f \dot{x}_e = (&v_l\cos\theta_l + D_l\omega_l\cos\theta_l - \rho_{1l}\cos\theta_l \\
&-\mu_l\sin\theta_l - D_l\rho_{2l}\cos\theta_l - v_f\cos\theta_f \\
&+\omega_f D_f\sin\theta_f + \rho_{1f}\cos\theta_f \\
&-\rho_{2f}D_f\sin\theta_f + \mu_f\sin\theta_f)\sin\theta_f,
\end{aligned} \tag{19}$$

$$\begin{aligned}
\cos\theta_f \dot{y}_e = (&v_l\sin\theta_l + D_l\omega_l\sin\theta_l - \rho_{1l}\sin\theta_l \\
&+\mu_l\cos\theta_l - D_l\rho_{2l}\sin\theta_l - v_f\sin\theta_f \\
&-\omega_f D_f\cos\theta_f + \rho_{1f}\sin\theta_f \\
&+\rho_{2f}D_f\cos\theta_f - \mu_f\cos\theta_f)\cos\theta_f.
\end{aligned} \tag{20}$$

From (19) and (20), ω_f is defined as

$$\omega_f = \frac{v_l}{D_f}\sin\theta_e + \frac{D_l\omega_l}{D_f}\sin\theta_e + f_1 + \rho_{2f}, \tag{21}$$

where

$$\begin{aligned}
f_1 = (&-\rho_{1l}\sin\theta_e + \mu_l\cos\theta_e - D_l\rho_{2l}\sin\theta_e - \mu_f \\
&+ \dot{x}_e\sin\theta_f - \dot{y}_e\cos\theta_f)/D_f.
\end{aligned}$$

Then, the dynamics of θ_e is derived as

$$\dot{\theta}_e = -\frac{v_l}{D_f}\sin\theta_e + f_2, \tag{22}$$

where $f_2 = (1 - (D_l/D_f)\sin\theta_e)\omega_l - f_1 - \rho_{2l}$ and $v_l/D_f > 0$. Since $\dot{x}_e$ and $\dot{y}_e$ are bounded, f_2 is bounded from Assumptions 1 and 2, that is, there exists a set Υ_{f_2} such that $f_2 \in \Upsilon_{f_2}$ where $t \ge 0$. Then, let us consider the positive definite function $\Omega = 1 - \cos\theta_e$. Substituting (22) into the time derivative of Ω, we have

$$\begin{aligned}
\dot{\Omega} &= -\frac{v_l}{D_f}\sin^2\theta_e + f_2\sin\theta_e \\
&\le -c_3\Omega + c_4,
\end{aligned} \tag{23}$$

where $c_3 = \min_{v_l \in \Upsilon_{v_l}} v_l/\eta_d$ and $c_4 = 2c_3 + \max_{f_2 \in \Upsilon_{f_2}} |f_2|$; Υ_{v_l} is a set satisfying $v_l \in \Upsilon_{v_l}$ where $t \ge 0$. Therefore, θ_e is bounded from (23).

From (21), we hold $(v_l + D_l w_l - D_l\rho_{2l} - \rho_{1l} + \mu_l)\sin\theta_e + D_f\rho_{2f} - D_f\omega_f - \mu_f = -\dot{x}_e\sin\theta_f + \dot{y}_e\cos\theta_f$. Since the derivatives of the point tracking errors $(\dot{x}_e, \dot{y}_e)$ can be reduced to an adjustable neighborhood of the origin, $\lim_{t\to\infty}[\sin\theta_e - (D_f\dot{\theta}_f + \mu_f)/(v_l + D_l\dot{\theta}_l - \rho_{1l} + \mu_l)] \le \varpi$ is satisfied. Here, we can see that if the follower robot does not rotate (i.e., $\dot{\theta}_f = 0$) and its lateral skidding velocity μ_f is $\mu_f = 0$, the orientation error θ_e converges to an adjustable neighborhood of the origin.

Remark 5: The previous papers [9-11] considering skidding and slipping effects require the accurate measurement of skidding and slipping using sensors, but use of sensors may cause the performance degradation because of sensor noise. In addition, the results [9-11] can be applied only to single mobile robots. However, the controller proposed in this paper does not require sensor information because the adaptive control technique (10) is employed to compensate unknown skidding and slipping effects in both the leader and the follower robots. Moreover, this study extends the unknown skidding and slipping problem to the formation control of multiple mobile robots.

Remark 6: In this paper, the obstacle avoidance problem in the leader-follower formation control is not considered. However, multiple obstacles commonly exist in real world applications. In future work, it will be interesting to address the leader-follower formation tracking problem by considering obstacle avoidance for multiple mobile robots in the presence of unknown skidding and slipping effects.

4. SIMULATION RESULTS

In this section, one leader and two followers are considered to demonstrate the effectiveness of the proposed control system in maintaining the desired formation under skidding and slipping effects. The matrices for the dynamic model of the leader and followers employed in this simulation have been taken from [35].

The initial postures for the leader and the two followers are $(x_l, y_l, \theta_l) = (0,0,0)$, $(x_{f1}, y_{f1}, \theta_{f1}) = (0, 4,$

0), and $(x_{f2}, y_{f2}, \theta_{f2}) = (0, -4, 0)$, respectively. The desired relative positions of the followers with respect to the leader are $\eta_{d,f1} = 2$ m, $\phi_{d,f1} = -\pi/3$ rad, and $\eta_{d,f2} = 2$ m, $\phi_{d,f2} = \pi/3$ rad, respectively. The velocity of the reference robot, which is used to generate the reference trajectory of the leader robot, is chosen as $v_r = 0.8$ m/s and $\omega_r = 0.07$ rad/s. With the aim of observing the performance of the proposed formation controller when the leader robot skids and slips, this robot is controlled by a controller designed without considering skidding and slipping as proposed in [36]. For practical purposes, we use the skidding and slipping effects that were measured experimentally in [37]. In other words, ρ_2 and μ are chosen as Gaussian random variables with mean 0.05 and standard deviation 0.03, and with mean 0 and standard deviation 0.03, respectively. Here, ρ_1 is set to zero. These skidding and slipping effects influence the leader and follower robots from $t = 20$ s to $t = 60$ s. In addition, we consider the measurement errors with Gaussian random variables as discussed in [37]. The controller parameters are chosen as $k = 1$, $r_1 = r_2 = 9$, $\sigma = 0.1$, $\varepsilon = 0.1$, and $\lambda_1 = \lambda_2 = 2$.

Fig. 2(a) shows the formation tracking result of the proposed control system. The tracking errors x_e and y_e are shown in Figs. 2(b) and 2(c), respectively. As shown in Fig. 2(d), the orientation errors of the follower robots are bounded and converge to $\theta_e \simeq \arcsin((D_f\dot{\theta}_f + \mu_f)/(v_l + D_l\dot{\theta}_l - \rho_{1l} + \mu_l)) = 5.9195°$ and $4.3578°$, respectively, as stated in Theorem 1. In addition, Figs. 2(e) and 2(f) show the tracking errors of the leader robot in the presence of the skidding and slipping effects. These figures reveal that the proposed adaptive formation control scheme can achieve the desired formation tracking regardless of the presence of unknown Gaussian skidding and slipping effects and the leader robot's skidding and slipping.

5. CONCLUSION

In this paper, an adaptive formation controller for mobile robots with unknown skidding and slipping has been presented. Virtual robots have been used to design the proposed control system instead of using actual robots, and the kinematics of the virtual robots has been derived in the presence of slipping and skidding effects. The adaptive formation controller for the derived robot model has been designed based on the leader-follower approach and the adaptive technique has been used to compensate unknown skidding and slipping effects. From the Lyapunov stability theorem, we have proved that all signals of the closed-loop system are uniformly ultimately bounded, and the point tracking errors for the desired formation also converge to an adjustable neighborhood of the origin. Thus, we can guarantee that the proposed formation control scheme maintains the desired formation successfully regardless of the presence of unknown skidding and slipping effects.

REFERENCES

[1] Z. P. Jiang and H. Nijmeijer, "Tracking control of mobile robots: a case study in backstepping," *Automatica*, vol. 33, no. 7, pp. 1393-1399, 1997.
[2] S. J. Yoo, Y. H. Choi, and J. B. Park, "Generalized predictive control based on self-recurrent wavelet neural network for stable path tracking of mobile robots: adaptive learning rates approach," *IEEE Trans. Circuit and Systems I*, vol. 53, no. 6, pp. 1381-1394, 2006.
[3] T. Fukao, H. Nakagawa, and N. Adachi, "Adaptive tracking control of a nonholonomic mobile robot," *IEEE Trans. Robot. Automat.*, vol. 16, no. 5, pp. 609-615, 2000.
[4] W. Dong and K. D. Kuhnert, "Robust adaptive control of nonholonomic mobile robot with parameter and nonparameter uncertainties," *IEEE Trans. Robotics*, vol. 21, no. 2, pp. 261-266, 2005.
[5] B. Park, S. J. Yoo, Y. H. Choi, and J. B. Park, "A simple adaptive control approach for trajectory tracking of nonholonomic electrically driven mobile robots," *IEEE Trans. Control Systems Technol.*, vol. 18, no. 5, pp. 1199-1206, 2010.
[6] W. E. Dixon, M. S. Queiroz, D. M. Dawson, and T. J. Flynn, "Adaptive tracking and regulation of a wheeled mobile robot with controller/update law modularity," *IEEE Trans. Contr. Syst. Technol.*, vol. 12, no. 1, pp. 138-147, 2004.
[7] K. D. Do, Z. P. Jiang, and J. Pan, "Simultaneous tracking and stabilization of mobile robots: an adaptive approach," *IEEE Trans. Autom. Control*, vol. 49, no. 7, pp. 1147-1152, 2004.
[8] Z. P. Wang, S. S. Ge, and T. H. Lee, "Adaptive neural network control of a wheeled mobile robot violating the pure nonholonomic constraint," *Proc. IEEE Int. Conf. Decision and Control*, pp. 5198-5203, 2004.
[9] F. Hamerlain, K. Achour, T. Floquet, and W. Perruquetti, "High order sliding mode control of wheeled mobile robots in the presence of sliding effects," *Proc. IEEE Conf. Decision and Control*, pp. 1959-1963, 2005.
[10] D. Wang and C. B. Low, "Modeling and analysis of skidding and slipping in wheeled mobile robots: Control design perspective," *IEEE Trans. Robotics*, vol. 24, no. 3, pp. 676-687, 2008.
[11] C. B. Low and D. Wang, "GPS-based path following control for a car-like wheeled mobile robot with skidding and slipping," *IEEE Trans. Control Systems Technol.*, vol. 16, no. 2, pp. 340-347, 2008.
[12] C. B. Low and D. Wang, "GPS-based tracking control for a car-like wheeled mobile robot with skidding and slipping," *IEEE Trans. Mechatronics*, vol. 13, no. 4, pp. 480-484, 2008.
[13] S. J. Yoo, "Adaptive tracking control for a class of wheeled mobile robots with unknown skidding and slipping," *IET Control Theory and Appl.*, vol. 4, no. 10, pp. 2109-2119, 2010.
[14] T. Balch and R. C. Arkin, "Behavior-based

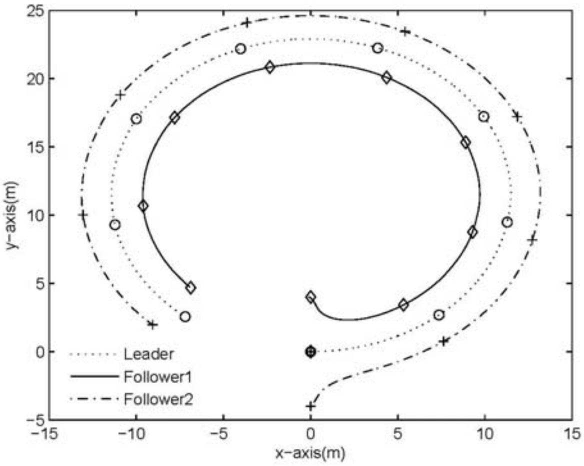

(a) Trajectory.

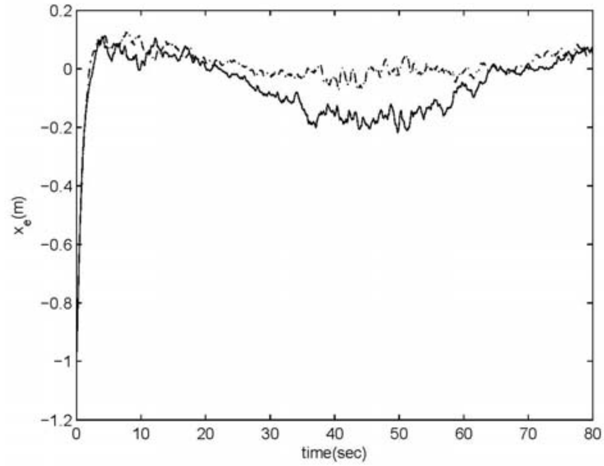

(b) x_e (solid : follower 1, dash-dot : follower 2).

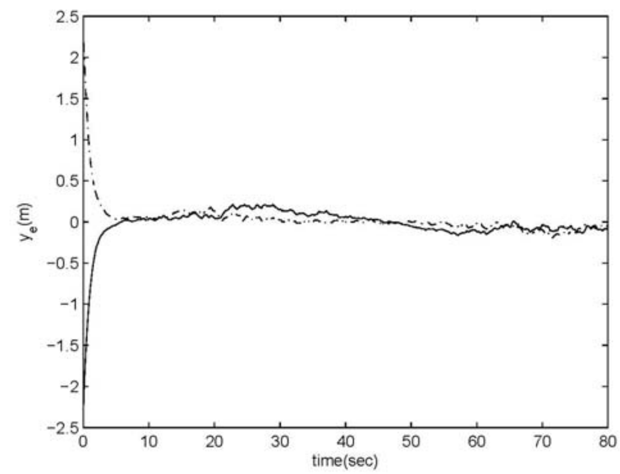

(c) y_e (solid : follower 1, dash-dot : follower 2).

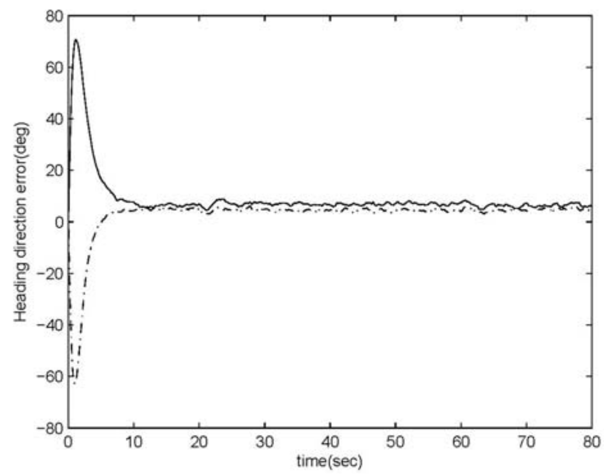

(d) θ_e (solid : follower 1, dash-dot : follower 2).

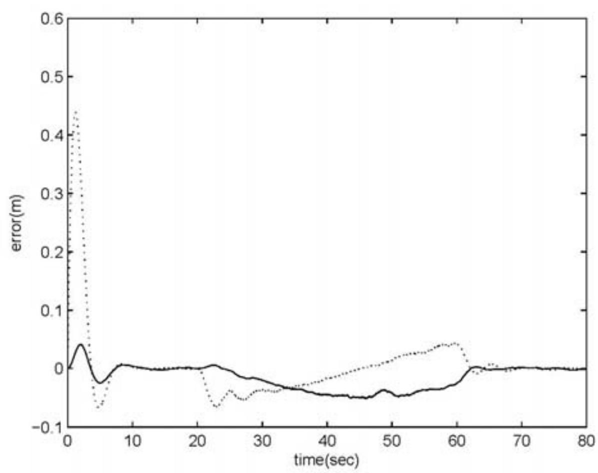

(e) The position errors of the leader robot (solid : x_l, dotted : y_l).

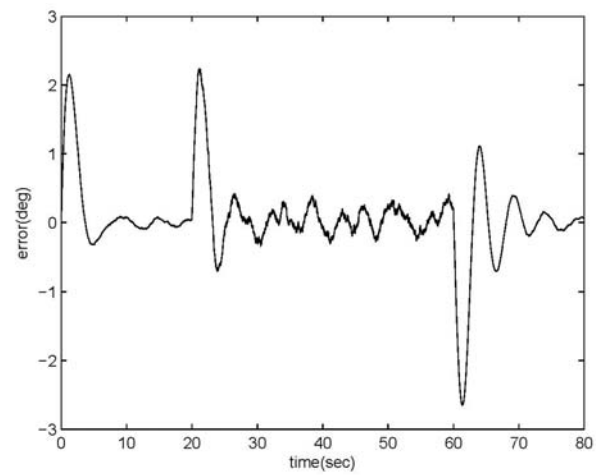

(f) The heading error of the leader robot.

Fig. 2. Formation control results and errors.

formation control for multiplerobot teams," *IEEE Trans. Robot. Automat.*, vol. 14, no. 6, pp. 926-939, 1998.

[15] J. Fredslund and M. J. Mataric, "A general algorithm for robot formations using local sensing and minimal communication," *IEEE Trans. Robot. Automat.*, vol. 18, no. 5, pp. 837-846, 2002.

[16] W. Ren and N. Sorensen, "Distributed coordination architecture for multi-robot formation control," *Robot. Auton. Syst.*, vol. 56, pp. 324-333, 2008.

[17] M. Ou, H. Du, and S. Li, "Finite-time formation control of multiple nonholonomic mobile robots," *Int. Journal of Robust and Nonlinear Control*, vol. 24, no. 1, pp. 140-165, 2014.

[18] M. A. Lewis and K. H. Tan, "High precision formation control of mobile robots using virtual structures," *Auton. Robots*, vol. 4, no. 4, pp. 387-403, 1997.
[19] S. J. Yoo, Y. H. Choi, and J. B. Park, "Adaptive formation tracking control of electrically driven multiple mobile robots," *IET Control Theory and Appl*., vol. 4, no. 8, pp. 1489-1500, 2010.
[20] Y. H. Lee, S. G. Kim, T. Y. Kuc, J. K. Park, S. H. Ji, Y. S. Moon, and Y. J. Cho, "Virtual target tracking of mobile robot and its application to formation control," *Int. Journal of Control, Automation, and Systems*, vol. 12, no. 2, pp. 390-398, 2014.
[21] J. P. Desai, J. Ostrowski, and V. Kumar, "Modeling and control of formations of nonholonomic mobile robots," *IEEE Trans. Robot. Automat*., vol. 17, no. 6, pp. 905-908, 2001.
[22] Z. Peng, G. Wen, A. Rahmani, and Y. Yu, "Leaderfollower formation control of nonholonomic mobile robots based on a bioinspired neurodynamic based approach," *Robot. Auton. Syst*., vol. 61, no. 9, pp. 988-996, 2013.
[23] J. Shao, G. Xie, and L. Wang, "Leader-following formation control of multiple mobile vehicles," *IET Control Theory Appl.*, vol. 1, no. 2, pp. 545-552, 2007.
[24] S. Mastellone, D. M. Stipanovic, C. R. Graunke, K. A. Intlekofer, and M. W. Spong, "Formation control and collision avoidance for multi-agent non-holonomic systems: Theory and experiments," *Int. J. Rob. Res*., vol. 27, no. 1, pp. 107-126, 2008.
[25] K. Choi, S. J. Yoo, J. B. Park, and Y. H. Choi, "Adaptive formation control in absence of leader's velocity information," *IET Control Theory Appl*., vol. 4, no. 4, pp. 521-528, 2010.
[26] T. Liu and Z. P. Jiang, "Distributed formation control of nonholonomic mobile robots without global position measurements," *Automatica*, vol. 49, no. 2, pp. 592-600, 2013.
[27] M. Defoort, T. Floquet, A. Kokosy, and W. Perruquetti, "Sliding-mode formation control for cooperative autonomous mobile robots," *IEEE Trans. Ind. Elec*., vol. 55, no. 11, pp. 3944-3953, 2008.
[28] B. S. Park, J. B. Park, and Y. H. Choi, "Robust formation control of electrically driven nonholonomic mobile robots via sliding mode technique," *Int. Journal of Control, Automation, and Systems*, vol. 9, no. 5, pp. 888-894, 2011.
[29] T. Dierks and S. Jaggannathan, "Neural network output feedback control of robot formations," *IEEE Trans. System, Man, and Cybern*., vol. 40, no. 2, pp. 383-399, 2010.
[30] T. Dierks, B. Brenner, and S. Jaggannathan, "Neural network-based optimal control of mobile robot formations with reduced information exchange," *IEEE Trans. Control Syst. Technol*., vol. 21, no. 4, pp. 1407-1415, 2013.
[31] J. Ghommam, H. Mehrjerdi, and M. Saad, "Robust formation control without velocity measurement of the leader robot," *Control Engineering Practice*, vol. 21, no. 8, pp. 1143-1156, 2013.
[32] B. S. Park, J. B. Park, and Y. H. Choi, "Adaptive formation control of electrically driven nonholonomic mobile robots with limited information," *IEEE Trans. System, Man, and Cybern*., vol. 41, no. 4, pp. 1061-1075, 2011.
[33] Y. D. Li, L. Zhu, and M. Sun, "Adaptive neural-network control of mobile robot formations including actuator dynamics," *Applied Mechanics and Materials*, vol. 303-306, pp. 1768-1773, 2013.
[34] P. A. Ioannou and P. V. Kokotovic, *Adaptive Systems with Reduced Models*, Springer-Verlag, New York, 1983.
[35] R. Fierro and F. L. Lewis, "Control of a nonholonomic mobile robot using neural networks," *IEEE Trans. Neural Networks*, vol. 9, no. 4, pp. 589-600, 1998.
[36] D. Chwa, "Sliding-mode tracking control of nonholonomic wheeled mobile robots in polar coordinates," *IEEE Trans. Control Syst. Technol*., vol. 12, no. 4, pp. 637-644, 2004.
[37] C. B. Low and D. Wang, "Maneuverability and path following control of wheeled mobile robot in the presence of wheel skidding and slipping," *Journal of Field Robotics*, vol. 27, no. 2, pp. 127-144, 2010.

Bong Seok Park received his B.S., M.S., and Ph.D. degrees in Electrical and Electronic Engineering from Yonsei University, in 2005, 2008, and 2011, respectively. Since 2012, he has been with the Department of Electronic Engineering, Chosun University, where he is currently an Assistant Professor. His research interests include nonlinear control, adaptive control, formation control, and the control of robots.

Sung Jin Yoo received his B.S., M.S., and Ph.D. degrees from Yonsei University, Seoul, Korea, in 2003, 2005, and 2009, respectively, in Electrical and Electronic Engineering. He has been a Post-doctoral researcher in the Department of Mechanical Science and Engineering, University of Illinois at Urbana-Champaign, Illinois from 2009 to 2010. He is currently an Assistant Professor in the School of Electrical and Electronics Engineering, Chung-Ang University, Seoul, Korea. His research interests include nonlinear adaptive control, decentralized control, distributed control, and neural networks theories, and their applications to robotic, flight, and time-delay systems.